

generated midgap levels, capacitance transients were nonexponential. The time-dependent capacitance waveforms were analyzed, computer fitted by three exponentials, and the evolution with temperature of these three time constants was studied. Thermal activation energies ranging from 0.65 eV (fast transient edge) to 0.8 eV (slow transient tail) were determined, and this result correlates with the detected broad DLTS bands at 0.7 eV (Fig. 1). The results for this computer analysis of the transient capacitance waveforms in $x = 0.85$ compositions are summarized in Fig. 2.

To study the presence of photocapacitance quenching due to the 0.7-eV band shown in Fig. 1, electrons in the original 0.27-eV level ($E_{I0} = 1.06$ eV) have to be pumped out before searching for photoquenching. Level E_{n2} was discharged thermally and by illuminating with 1.4 eV photons, and afterwards the photocapacitance was studied under a near 1.0-eV light (just below the optical threshold for E_{n2} and inside the reported photoquenching spectrum for GaAs). Photocapacitance quenching was detected, as shown in Fig. 3, although its efficiency was lower as x increases, in agreement with the results of Omling *et al.* for native EL2 in MOCVD GaAsP samples.⁹ The spectral distribution for the quenching effect is shown in Fig. 3 and agrees with the 1.0–1.4 eV range found for the EL2–EL2* transition in GaAs.^{3,9}

The generation rate for such proposed EL2-related levels is 1 center cm^{-1} per incident neutron. This result can be compared with a rate of $\sim 10 \text{ cm}^{-1}$ neutron for $\text{As}_{\text{Ga}}^{4+}$ centers determined by EPR in neutron irradiated GaAs for similar neutron dose.^{10,11}

Thermal and electron-induced regeneration of the EL2* metastable state has been described in GaAs and in $x < 0.08$ $\text{GaAs}_{1-x}\text{P}_x$ alloys.⁹ Again, the presence of other native deep levels disturb quantitative measurements, as indicated also by Omling *et al.*⁹ Electron regeneration was found in all samples studied and this effect was used for the isothermal photocapacitance quenching studies described in Fig. 3. Concerning thermal regeneration, the present data indicate that the temperature range to detect quenching effects ex-

tends to higher temperatures as x increases.

In conclusion, we have shown in this work that fast neutron irradiated samples, annealed at room temperature, generate a broad band at about 0.7 eV, having a multilevel structure, as determined by computer analysis. It has been proposed this generated defect belongs to the EL2 family because the presence of photocapacitance quenching effects in a photon spectrum usually assigned to the EL2 center. Results are explained through neutrons creating clusters and point defect complexes that include the EL2 defect structure.

The present results extend to GaAsP alloys the results of Martin *et al.* and Magno *et al.* concerning neutron irradiated LEC, liquid phase epitaxy (LPE), and HB GaAs, although they did not report photoquenching experiments.^{5,6}

We thank Dr. F. Kellert, Hewlett-Packard Optoelectronics Division, for providing samples, and Juan Martinez for his technical assistance concerning the DLTS system. This work has been partially supported by Instituto de Estudios Nucleares and by Comisión Asesora de Investigación Científica y Técnica, projects 3864/79 and 1437/82.

¹G. M. Martin, J. P. Farges, G. Jacob, and J. P. Hallais, *J. Appl. Phys.* **51**, 2840 (1980).

²T. Ikoma, M. Takikawa, and M. Taniguchi, *Inst. Phys. Conf. Ser.* **63**, 191 (1982).

³T. Ikoma, M. Taniguchi, and Y. Mochizuki, *International Symposium on GaAs and Related Compounds*, Biarritz, France 1984.

⁴B. K. Meyer, J. M. Spaeth, and M. Scheffer, *Phys. Rev. Lett.* **52**, 851 (1984).

⁵R. Magno, J. G. Giessner, and M. Spencer, *International Conference on Defects in Semiconductors*, Coronado 1984.

⁶G. M. Martin, E. Esteve, P. Langlade, and S. Makram-Ebeid, *J. Appl. Phys.* **56**, 2655 (1984).

⁷E. Calleja, E. Muñoz, and F. García, *Appl. Phys. Lett.* **42**, 528 (1983).

⁸E. Calleja, E. Muñoz, B. Jiménez, A. Gómez, F. García, and F. Kellert, *J. Appl. Phys.* **57**, 5295 (1985).

⁹P. Omling, L. Samuelson, and H. G. Grimmeis, *Phys. Rev. B* **29**, 4534 (1984).

¹⁰E. R. Weber (private communication).

¹¹A. Goltzene, B. Meyer, C. Schwab, S. G. Greenbaum, and R. J. Wagner, *Proceedings of International Symposium on GaAs and Related Compounds*, Biarritz, France 1984.

Dominant moving species in the formation of amorphous NiZr by solid-state reaction

Y.-T. Cheng, W. L. Johnson, and M.-A. Nicolet
California Institute of Technology, Pasadena, California 91125

(Received 17 June 1985; accepted for publication 5 August 1985)

The displacements of W and Hf markers have been monitored by backscattering of MeV He to study the growth of the amorphous NiZr phase by solid-state reaction. We find that the Ni is the dominant moving species in this reaction.

Amorphous metallic alloys have been traditionally produced by rapid quenching from the melt or by sputtering.¹ Recently, however, it has been demonstrated that the amorphous metallic phase can also be produced by solid-state

reaction.^{2–8} The energetic and kinetic requirements for such a reaction to occur seem to be a compromise between a lowering of the free energy, and a mode of growth that favors the amorphous phase over the crystalline ones.⁶ Detailed kinetic

studies are still lacking. In this letter we attempt to identify the dominant moving species during such a reaction in the Ni-Zr system. The amorphization of Ni/Zr bilayers by solid-state reaction has been previously reported by several research groups.^{4,7}

In their original diffusion experiments Kirkendall and Smigelskas used Mo wires ($\sim 10 \mu\text{m}$ in diameter) as markers between two bulk metals, to determine which of the latter had the greater intrinsic diffusion coefficient.⁹ In thin-film diffusion studies, with film thicknesses of the order 1000 Å, inert markers that fulfill an equivalent function must be very thin ($< 10 \text{ Å}$). They can be realized by either evaporation or ion implantation. The positional change of the marker as well as the thickness of the growing amorphous layer may be monitored by MeV backscattering spectrometry (BS).¹⁰ Thus the dominant moving species is determined by studying such small scale Kirkendall effect. Details of this kind of marker experiments may be found in literature relating to silicide formation.¹¹⁻¹⁶

The sample configuration is shown in Fig. 1 (insert). W and Hf were selected as markers because of their heavy atomic mass, so that their BS signal would separate from those of Zr and Ni. Furthermore, W may be considered an "inert" marker, whereas Hf is an "isotope" of Zr (detailed discussion below). About 4-10 Å of marker material were deposited. The top Zr layer thickness was optimized to allow a substantial amount of Zr to react while avoiding an overlap of the 2 MeV $^4\text{He}^+$ backscattering signals from Zr and from the marker. A thickness of 500-1000 Å for the Zr layer was found appropriate. The Ni layer thickness was about 1600 Å. The thin layers of Ni and Zr ($\sim 25 \text{ Å}$) on either side of the marker were used in some cases so as to position the marker within amorphous NiZr after an initial short thermal annealing step. This configuration is advantageous to minimize the possible influence of interfaces on the movement of the marker ("interfacial drag").¹⁵ For some samples, a thin layer of Zr was also deposited between the Ni film and the SiO_2 substrate to improve adhesion.

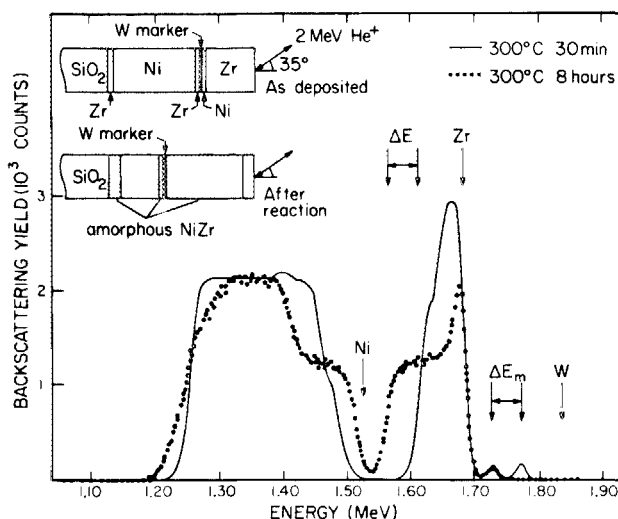


FIG. 1. 2.0 MeV 35°He^+ backscattering spectra of a Ni-W (4 Å)-Zr sample (insert) annealed for 30 min and 8 h at 300 °C. The displacement of the marker peak position and of the Ni-amorphous NiZr interface half-height position, are shown by ΔE_m and ΔE , respectively. The spectra were taken with 1.66 keV/channel.

Samples were prepared by electron gun evaporation from metallic targets onto oxidized silicon substrates. The vacuum in the evaporator chamber was in the 10^{-8} Torr range prior to deposition, and below 2×10^{-7} Torr during evaporation. The layer thicknesses were measured *in situ* by a quartz crystal thickness monitor, and subsequently by BS. The films were thermally treated at $300 \pm 1 \text{ °C}$ after being removed from the evaporation chamber (amorphous NiZr forms in the range of 250-350 °C by solid-state reaction⁷). The vacuum in the annealing furnace was kept below 8×10^{-7} Torr. The depth profile of the films was recorded at different stages of thermal annealing by BS using 2 MeV $^4\text{He}^+$ ions. Care was taken to keep the intensity of the analyzing beam sufficiently low so as not to cause substantial heating of the samples. Selected samples were checked by x-ray diffraction (Read camera and Philips theta-two theta vertical diffractometer using $\text{Cu } K_\alpha$ radiation). The as-deposited Ni and Zr were both highly textured polycrystalline materials with preferred growth normal to close packed planes, that is, $\langle 111 \rangle$ in Ni and $\langle 002 \rangle$ in Zr. The average grain sizes were about 280 Å (Ni $\langle 111 \rangle$) and 190 Å (Zr $\langle 002 \rangle$) in diameter for Ni and Zr, respectively. Amorphous halos were observed after thermal treatment, as expected.

Backscattering spectra of a Ni-Zr sample with a W ($\sim 4 \text{ Å}$) marker annealed for 30 min and 8 h at 300 °C are shown in Fig. 1. The reaction reached completion after the 8 h of annealing. The residual nonreacted Zr near the surface (see Fig. 1) was probably caused by oxidation during the thermal annealing.⁵ The movement of the W marker signal towards decreasing energy is apparent. During the initial 30 min of annealing, the thin layers ($\sim 25 \text{ Å}$) of Ni and Zr on either side of W react, so that the marker is then positioned within the amorphous NiZr. Beyond this preannealing step, the energy displacement of the marker signal, ΔE_m , is equal to the displacement of the Ni-amorphous NiZr interface, ΔE (see Figs. 1 and 2), within the experimental uncertainty. The en-

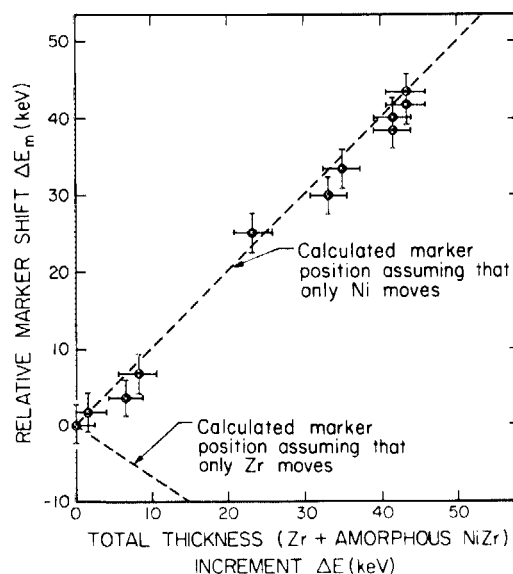


FIG. 2. Amount of displacement of the W marker, ΔE_m , vs the amount of displacement of the Ni-amorphous NiZr interface, ΔE . Both quantities are measured relative to those of the sample annealed for 30 min at 300 °C (see Fig. 1). The two dashed lines correspond to the energy shift of the W marker under the assumption that either Ni or Zr is the only diffusing species.

ergy shifts ΔE_m and ΔE were determined by measuring the peak position of the W marker signal for ΔE_m , and the position of the half-height of the low-energy edge of the Zr signal for ΔE . Both ΔE_m and ΔE were measured relative to those of the sample annealed for 30 min at 300 °C. To first order, the equal amount of downward shift in energy of ΔE_m and ΔE indicates that the energy shifts are due to Ni diffusing through W marker and into amorphous NiZr in distance space. Therefore, Ni is the only moving species in amorphous NiZr formation by solid-state reaction.

After the first 30 min preannealing and before the reaction nears completion, the shift of the marker was observed to be roughly proportional to $t^{1/2}$. The $t^{1/2}$ growth behavior is in accordance with an earlier x-ray intensity study of the amorphous phase growth kinetics by solid-state reaction for the NiZr system.⁷ We have also established that the outcome of the experiment (i.e., Fig. 2) does not change if the amount of W used as the marker is doubled.

W has also been used as a marker to determine the dominant moving species in Ni silicide formation.¹⁶ The results of these experiments agree with marker experiments using a chemically inert marker such as Xe.¹¹ In fact, W has a heat of mixing close to zero with both Ni and Zr.¹⁷ Therefore, W is quite likely an inert marker for Ni-Zr diffusion studies, but it would be desirable to support this contention by additional independent measurements.

In a second set of experiments, we selected Hf as the marker instead of W. Many physical and chemical properties of Hf are very similar to those of Zr. Hf and Zr are both from the IV B group of the periodic table of the elements. As pure metals, they have the same hcp crystal structure in the temperature range considered as well as nearly identical Goldschmidt radii. Moreover, they form a continuous solid solution across the entire compositional range.¹⁸ Like Ni/Zr, Ni/Hf bilayers form amorphous alloys by solid-state reaction at temperatures between 290 and 380 °C.⁵ Therefore, Hf may be considered as a nearly ideal isoelectronic substitute of Zr in the context of this diffusion study. Assuming that this is so, if Ni is the only moving species in amorphous NiZr formation, there is no movement of Zr with respect to itself, so that there should be no movement of Hf with respect to Zr either. As a result, the position of the Hf marker relative to the growing amorphous layer should be the same as that of the W marker (Figs. 1 and 2). Furthermore, the BS signal of the Hf marker should remain sharp as does the W signal, except for some small spreading of the marker signal due to the increase of energy straggling as more Ni accumu-

lates above the marker.¹⁰ All these expected features have been observed experimentally. The shift of the marker was observed to increase linearly with $t^{1/2}$ beyond the first 1 h of annealing.

In conclusion, the "inert" and "isotopic" marker experiments show that Ni is the moving element in the amorphous NiZr formation by solid-state reaction. We believe that a general feature of the metallic amorphous phase formed by solid-state reaction is that one species moves predominantly during the amorphous phase formation. Further studies are under way.

The authors would like to thank D. Groseth and A. Ghaffari for sample preparations. Many discussions with W. J. Meng, Dr. K. M. Unruh, M. Atzmon, T. Banwell, F. C. T. So, and Dr. M. Van Rossum have been very helpful. Partial financial support was provided by the Office of Naval Research under contract No. N00014-84-IL-0275 and the Department of Energy under contract No. DE-AA03-76SF00767.

¹R. Zallen, *The Physics of Amorphous Solids* (Wiley, New York, 1983), p. 5.

²R. B. Schwarz and W. L. Johnson, *Phys. Rev. Lett.* **51**, 415 (1983).

³R. B. Schwarz, K. L. Wang, W. L. Johnson, and B. M. Clemens, *J. Non-Cryst. Solids* **61 & 62**, 129 (1984).

⁴B. M. Clemens, W. L. Johnson, and R. B. Schwarz, *J. Non-Cryst. Solids* **61 & 62**, 817 (1984).

⁵M. Van Rossum, M-A. Nicolet, and W. L. Johnson, *Phys. Rev. B* **29**, 5498 (1984).

⁶W. L. Johnson, B. P. Dolgin, and M. Van Rossum, in *Glass...Current Issues*, edited by A. F. Wright and J. Dupuy (NATO ASI Series, Martinus Nijhoff, Dordrecht, Boston, Lancaster, 1984), p. 172.

⁷K. M. Unruh, W. J. Meng, and W. L. Johnson, in *Materials Research Society Symposium Proceedings*, edited by J. M. Gibson and L. R. Dawson (Materials Research Society, Pittsburgh, 1985), Vol. 37, p. 551.

⁸P. Guilmin, P. Guyot, and G. Marchal, *Phys. Lett. A* **109**, 174 (1985).

⁹A. D. Smigelskas and E. D. Kirkendall, *Trans. Am. Inst. Min. Engrs.* **171**, 130 (1947).

¹⁰W. K. Chu, J. W. Mayer, and M-A. Nicolet, *Backscattering Spectrometry* (Academic, New York, San Francisco, London, 1978).

¹¹W. K. Chu, H. Krautle, J. W. Mayer, M-A. Nicolet, and K. N. Tu, *Appl. Phys. Lett.* **25**, 454 (1974).

¹²G. J. van Gorp, D. Sigurd, and W. F. van der Weg, *Appl. Phys. Lett.* **29**, 159 (1976).

¹³R. Pretorius, L. L. Ramiller, S. S. Lau, and M-A. Nicolet, *Appl. Phys. Lett.* **30**, 501 (1977).

¹⁴J. Baglin, F. d'Heurle, and S. Peterson, *Appl. Phys. Lett.* **33**, 289 (1978).

¹⁵K. N. Tu and J. W. Mayer, in *Thin Films, Interaction and Reactions*, edited by J. M. Poate, K. N. Tu, and J. W. Mayer (Wiley, New York, 1978), Chap. 10.

¹⁶K. Affolter, X. A. Zhao, and M-A. Nicolet, *J. Appl. Phys.* **58**, 3087 (1985).

¹⁷A. R. Miedema, *Philips Tech. Rev.* **36**, 217 (1976).

¹⁸M. Hanson and K. Anderko, *Constitution of Binary Alloys* (McGraw-Hill, New York, Toronto, London, 1958), p. 815.